Fluxgate magnetorelaxometry for characterization of hydrogel polymerization kinetics and physical entrapment capacity

2008 J. Phys.: Condens. Matter 20 204106

(http://iopscience.iop.org/0953-8984/20/20/204106)

J. Phys.: Condens. Matter **20** (2008) 204106 (5pp) doi:10.1088/0953-8984/20/20/204106

Fluxgate magnetorelaxometry for characterization of hydrogel polymerization kinetics and physical entrapment capacity

E Heim[1], S Harling[2], F Ludwig[1], H Menzel[2] and M Schilling[1]

[1] Institut für Elektrische Messtechnik und Grundlagen der Elektrotechnik, TU Braunschweig, Hans-Sommer-Straße 66, 38106 Braunschweig, Germany
[2] Institut für Technische Chemie, TU Braunschweig, Hans-Sommer-Straße 10, 38106 Braunschweig, Germany

E-mail: e.heim@tu-bs.de

Received 31 March 2008
Published 1 May 2008
Online at stacks.iop.org/JPhysCM/20/204106

Abstract
Hydrogels have the potential for providing drug delivery systems with long release rates. The polymerization kinetics and the physical entrapment capacity of photo-cross-linked hydroxyethyl methacrylate hydroxyethylstarch hydrogels are investigated with a non-destructive method. For this purpose, superparamagnetic nanoparticles as replacements for biomolecules are used as probes. By analyzing their magnetic relaxation behavior, the amounts of physically entrapped and mobile nanoparticles can be determined. The hydrogels were loaded with five different concentrations of nanoparticles. Different methods of analysis of the relaxation curves and the influence of the microviscosity are discussed. This investigation allows one to optimize the UV light irradiation time and to determine the amount of physically entrapped nanoparticles in the hydrogel network. It was found that the polymerization kinetics is faster for decreasing nanoparticle concentration but not all nanoparticles can be physically entrapped in the network.

1. Introduction

Hydrogels are under investigation for providing new drug delivery systems for bioactive molecules. They have the ability to incorporate a huge amount of water or buffer. Therefore, they offer optimal conditions for long *in vivo* lifetimes of, e.g., proteins. For hydrogels there exist different preparation methods and release mechanisms [2, 3]. Stimuli-sensitive hydrogels are able to react to environmental changes like temperature or pH value variations by altering their physical properties. Common characterization methods, e.g., swelling or rheology measurements, require a certain stiffness and a particular shape of the hydrogel. Biomolecules loaded during hydrogel polymerization can either become incorporated into the hydrogel network or remain in the hydrogel pores. The release time profiles depend on these two loading types. Before physically entrapped biomolecules can diffuse out of the hydrogel the network has to degrade, thus retarding their release rate. Recently, we have introduced a new non-destructive characterization method for hydrogels based on the relaxation behavior of superparamagnetic nanoparticles (MNP) [1]. Using MNPs as probes, the cross-linking state of the hydrogel can be measured at every stage. The microviscosity of the hydrogel solution can be determined in the early stages of the cross-linking where no MNPs are immobilized. The polymerization kinetics and the ratio of incorporated to mobile MNPs should be mainly influenced by the size of the drug as release studies suggest [4]. Therefore, the size of the MNPs should be of the order of the desired biomolecules. In addition, the shell of the MNPs must not polymerize itself during the polymerization process. In the following, five different concentrations of MNPs are used to determine the polymerization kinetics and physical entrapment capacity of the hydrogel investigated.

Table 1. Stability tests of ferrofluids with different shell materials. Agglomeration criteria for visually inspected relaxation curves: stable: no change in curves, slightly unstable: marginally increased time constants of curves, unstable: significantly increased time constants of curves.

Ferrofluid	Shell	Photo-initiator	UV irradiated water	UV irradiated photo-initiator
FluidMAG GA/GV	Gum arabic	Stable	Stable	Stable
FluidMAG-D	Starch monolayer	Stable	Slightly unstable	Slightly unstable
FluidMAG-D/5E	Starch multilayer	Stable	Stable	Unstable
FluidMAG–citrate	Citrate	Stable	Unstable	Unstable
DDM128N	Carboxy-dextran	Stable	Stable	Unstable

2. Methods

In magnetorelaxometry (MRX) experiments the time evolution of the net magnetization of the sample is measured after abruptly switching off a magnetizing field. In this work, the relaxation signals were measured with a MRX system based on a differential fluxgate magnetometer setup described in [5]. The measured net magnetization of the sample decays over time via two mechanisms: the Brownian rotation of the whole mobile MNP and the Néel relaxation of the inner magnetic moment. The relaxation of a polydisperse ensemble of mobile MNPs can be phenomenologically described by a stretched exponential function [6, 7]:

$$B(t) = B_{\mathrm{off}} + B_{\mathrm{mobile}} \exp\left(-\left(\frac{t}{\tau_{\mathrm{mobile}}}\right)^{\beta}\right). \qquad (1)$$

Here, the quantities τ_{mobile} and β are characteristic for a given ferrofluid and do not depend on the MNP concentration [7]. These quantities can in principle be determined from measurements on a reference sample containing only mobile MNPs. However, since the Brownian relaxation time constant τ_{B} is proportional to the viscosity of the medium, the phenomenological time constant τ_{mobile} also depends on it. The amplitude B_{mobile} is a measure of the mobile MNP fraction of the sample but—as systematic studies on the influence of the viscosity have shown—if the viscosity of the surrounding medium is changed, the phenomenological amplitude B_{mobile} also changes even for the same amount of mobile MNPs. The relaxation of an ensemble of immobilized MNPs can be described by the following function [5]:

$$B(t) = B_{\mathrm{off}} + B_{\mathrm{immobilized}} \ln\left(1 + \frac{\tau_{\mathrm{immobilized}}}{t}\right). \qquad (2)$$

The quantity $\tau_{\mathrm{immobilized}}$ is for small fields of the order of the magnetization time [8] and slightly varies from ferrofluid to ferrofluid, but it is independent of the surrounding medium. This parameter is determined from measurements on a reference sample where the MNPs were immobilized, e.g., by freeze drying in mannite solution. The amplitude $B_{\mathrm{immobilized}}$ is a measure of the immobilized MNP fraction of the sample. To quantify the binding kinetics, the relaxation curves can be analyzed as a superposition of the two mechanisms:

$$B(t) = B_{\mathrm{off}} + B_{\mathrm{mobile}} \exp\left(-\left(\frac{t}{\tau_{\mathrm{mobile}}}\right)^{\beta}\right) + B_{\mathrm{immobilized}} \ln\left(1 + \frac{\tau_{\mathrm{immobilized}}}{t}\right). \qquad (3)$$

3. Materials

3.1. Hydrogels

Photo-cross-linked hydrogels of hydroxyethyl methacrylate hydroxyethylstarch (HESHEMA) were investigated. HESHEMA was synthesized by modification of hydroxyethylstarch (HES) with hydroxyethyl methacrylate (HEMA) to introduce photo-cross-linkable functions along the polysaccharide backbone. Details are described in [1]. To obtain photo-cross-linked HESHEMA hydrogels, HESHEMA (10 wt%) with a degree of substitution of 0.07 was dissolved in an aqueous photo-initiator (0.1 wt% Irgacure 2959, Ciba Specialty Chemicals, Basel, Switzerland). Photo-cross-linking was carried out by irradiation with UV light ($\lambda = 366$ nm, $I \sim 3.5$ W cm^{-2}).

3.2. Superparamagnetic nanoparticles

Superparamagnetic nanoparticles for biomagnetic applications generally consist of a magnetic core and a shell protecting the core from chemical modification. In addition, the shell defines the functionality of the MNPs. For biomedical applications based on magnetorelaxometry, superparamagnetic nanoparticles are needed whose Néel relaxation time is longer than the Brownian one. This allows one to distinguish between immobilized and mobile MNPs. The critical MNP size for this condition depends on the magnetic material—e.g., at room temperature this core diameter for magnetite is of the order of 20 nm.

For the use as hydrogel probes, the MNP including shell should have about the same size as the target biomolecule and should be only physically incorporated in the network of the hydrogel. The MNPs should neither agglomerate in the photo-initiator, by UV light irradiation, nor in the UV light irradiated photo-initiator. In table 1 the results for different ferrofluids (chemicell GmbH, Germany, and Meito Sangyo, Japan) tested with the MRX system are listed. All ferrofluids are water based and the MNPs have an iron oxide core. As can be seen, fluidMAG GA/GV having a gum arabic shell is an appropriate ferrofluid because it exhibits no agglomeration in the three relevant tests. The tests were performed over a period of 45 min. For the ferrofluid fluidMAG GA/GV the tests were repeated up to a duration of 75 min. The hydrodynamic diameter measured by photon-correlation spectroscopy is about 50 nm and the solid concentration amounts to 75 mg ml^{-1}.

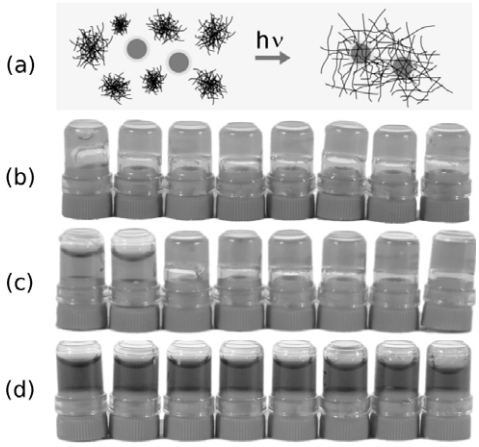

Figure 1. (a) Schematic of the hydrogel formation. Vial inversion tests from 5 to 40 min irradiation time for (b) hydrogel series I, (c) hydrogel series II, (d) hydrogel series V.

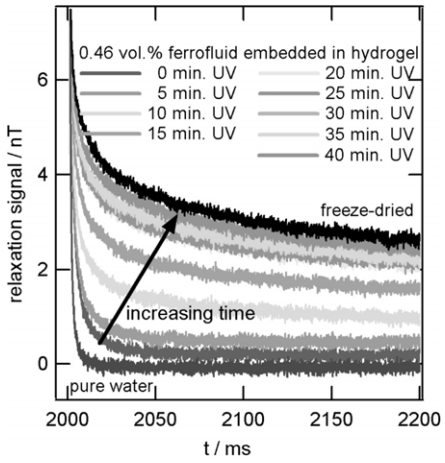

Figure 2. Relaxation curves of hydrogel series II.

Table 2. Hydrogel series names and properties related to 150 μl hydrogel.

Hydrogel series	Ferrofluid content (μl)	Ferrofluid content (vol%)	MNP content (vol%)
I	0.4	0.27	0.0038
II	0.7	0.46	0.0067
III	1.2	0.79	0.0114
IV	1.8	1.19	0.0171
V	2.4	1.57	0.0227

3.3. Superparamagnetic nanoparticle loaded hydrogels

Five HESHEMA hydrogel series were prepared with increasing ferrofluid content ranging from 0.46 to 1.57 vol%. In table 2 the sample parameters are listed. The amount of ferrofluid was added to 150 μl hydrogel solution in a microtiter vial (nunc-Immuno, BreakApart, Polysorp). Each series consists of eight samples which were consecutively irradiated with increasing time in 5 min steps. Measurements on the samples were subsequently made with the MRX system. In figure 1(a) a schematic of the hydrogel formation incorporating MNPs is visualized. The MNPs are suspended in an unirradiated HESHEMA hydrogel solution and are consecutively physically entrapped during the photo-polymerization.

4. Experimental results and discussion

4.1. Binding kinetics

In figures 1(b)–(d) photographs of the vial inversion test of the hydrogel series I, II and V are shown. Here the sample vials are turned over and a first criterion for having a hydrogel is that the substance remains at the bottom of the vial. For hydrogel series I, a gel is formed after 10 min of irradiation whereas for the hydrogel series V no gel is seen even after 40 min. Figure 2 shows the temporal evolution of the relaxation signal on increasing the UV light irradiation time for the samples in hydrogel series II in 5 min steps. In addition, the relaxation curves of a water diluted sample as well as of two reference samples with MNPs diluted in unirradiated hydrogel solution and with MNPs diluted in mannite solution and immobilized by freeze drying are depicted. For all other hydrogel series analogous measurements were performed in the same manner. Before analyzing the individual relaxation curves, the characteristic parameters are determined from reference samples. For each MNP concentration, one mobile and one immobilized reference sample was prepared. Each reference sample was fitted with the corresponding equations (1) and (2), respectively. The values B_{mobile}, τ_{mobile} and β were determined for reference samples with MNPs diluted in hydrogel solution without UV irradiation. In order to eliminate pipetting errors which influence the exact MNP content in the individual samples, a linear regression analysis was performed for the B_{mobile} and $B_{\mathrm{immobilized}}$ values of the reference samples as a function of nominal MNP concentration. The following expressions for the best linear regression fits were obtained: $B_{\mathrm{mobile}} = x\,(82.88 \pm 4.02)$ nT and $B_{\mathrm{immobilized}} = x\,(1.0068 \pm 0.0261)$ nT. The τ_{mobile}, β and $\tau_{\mathrm{immobilized}}$ values are averaged values from all corresponding reference samples: $\tau_{\mathrm{mobile}} = (48.61 \pm 19.85)$ μs, $\beta = 0.261 \pm 0.013$ and $\tau_{\mathrm{immobilized}} = (1300.34 \pm 0.14)$ ms.

Next, the relaxation curves of the five hydrogel series are fitted with (3) under the following four conditions, where the parameter β is always held constant:

- Method 1: τ_{mobile} is held constant and both amplitudes, normalized to the corresponding reference sample values, are constrained to 100%.
- Method 2: τ_{mobile} is held constant; no constraint on either amplitude.
- Method 3: τ_{mobile} is used a free fitting parameter; both amplitudes, normalized to the corresponding reference sample values, are constrained to 100%.
- Method 4: no constraints on amplitudes or τ_{mobile}.

Figure 3 depicts the fractions of mobile and immobilized MNPs for hydrogel series II depending on the irradiation time for the four analysis methods. It is noticeable that the calculated fractions of the immobilized MNPs coincide

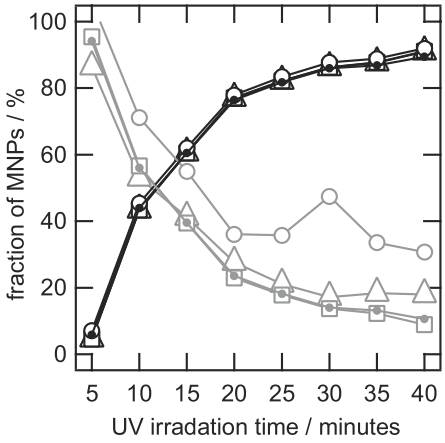

Figure 3. Formation kinetics and fractions of physically entrapped (black curves) and mobile (gray curves) MNPs for hydrogel series II. Fractions are shown for different analysis methods. □ method 1, △ method 2, ● method 3, ○ method 4.

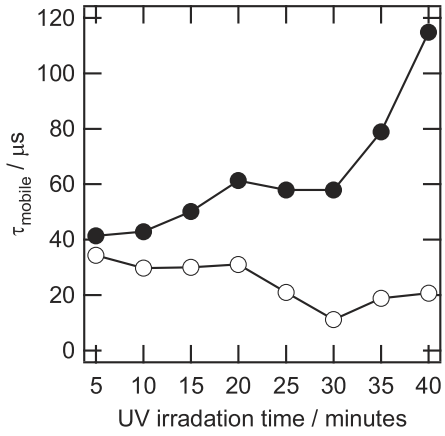

Figure 4. Evolution of the parameter τ_{mobile} for hydrogel series II. ● analysis method 3, ○ analysis method 4.

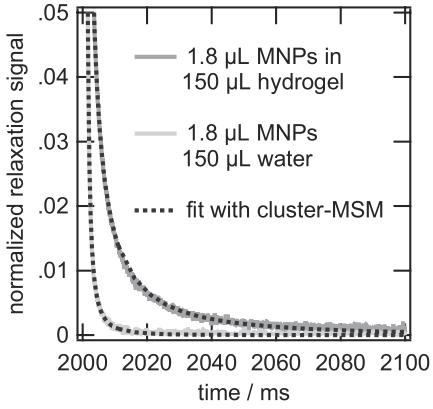

Figure 5. Relaxation curves of MNPs diluted in water and in unirradiated hydrogel solution, revealing the effect of changing microviscosity.

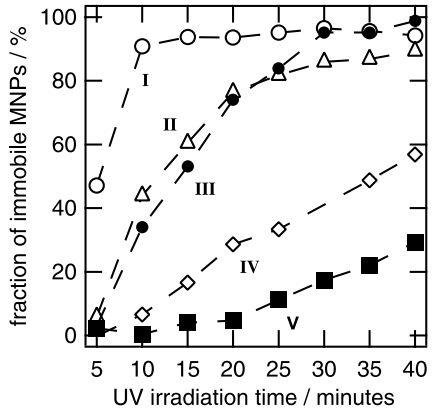

Figure 6. Polymerization kinetics for all hydrogel series.

whereas the values of the mobile fractions differ for the individual methods. For all other hydrogel series the same behavior is observed. An obvious reason is that the hydrogel changes its viscosity during the photo-cross-linking which is reflected in the phenomenological quantities τ_{mobile} and B_{mobile}. If, as in methods 1 and 2, τ_{mobile} is held constant, this will influence the value of B_{mobile}. Figure 4 shows the evolution of the time constant τ_{mobile} in the hydrogel series II for methods 3 and 4. It can clearly be seen that the temporal evolution significantly differs; the result from method 3 rather corresponds to the expectations. However, a clear decision can only be made on the basis of an analysis within the cluster moment superposition model (cluster-MSM) [9, 10].

To illustrate this, figure 5 shows the relaxation curves of MNPs diluted in water and of an unirradiated hydrogel solution. The two samples contain the same amount of MNPs. With the known viscosity of water of 1 mPa s at 20 °C the water diluted reference curve is fitted with the cluster MSM. The calculated mean hydrodynamic diameter is 75 nm. To determine the viscosity of the unirradiated hydrogel solution, its relaxation curve is fitted with the same size distribution parameters, yielding a viscosity 4.5 mPa s. Systematic studies of water–glycerine mixtures have shown that the viscosity measurements using conventional rheology and the microviscosity measurement using MRX yield the same results [10]. However, fitting the two relaxation curves with the phenomenological equation (1), τ_{mobile} for the hydrogel sample exceeds that for the aqueous one by a factor of 9 while B_{mobile} is a factor of 1.7 lower. This clearly indicates that one has to act with caution when analyzing binding kinetics with (3).

Figure 6 shows the immobilized MNP fractions for all hydrogel series. They were calculated for all series with method 3 as described for hydrogel series II. For the low-concentration hydrogel series I, the photo-polymerization saturated after 40 min and incorporates about 86% of the MNPs. In contrast the photo-polymerization of the high-concentration hydrogel series V did not saturate even after 40 min; at this time about 34% of the MNPs were incorporated. The hydrogel series I–III incorporate nearly, but not 100% of the MNPs. This could be due to pores or ducts in the micrometer regime resulting from phase separations during the formation of the hydrogel [11]. However, the amount of embedded MNPs for the first three hydrogel series I, II and III saturates whereas it does not for hydrogel series IV even

after 40 min. Therefore, the maximum entrapment capacity for this time range lies between those of the hydrogel series III and IV, leading to a guaranteed entrapment capacity of 0.79 vol% ferrofluid or 0.0114 vol% MNPs, respectively. The two hydrogel series IV and V did not saturate after a UV irradiation time of 40 min. Further investigations have shown that even after 75 min of UV irradiation the vial inversion test shows an unstable hydrogel. The progress of the cross-linking is obviously influenced by the irradiation time and the concentration of the MNP probes. The latter might influence the hydrogel formation since the MNPs also absorb UV light.

5. Summary and outlook

The measurements have shown that the polymerization kinetics and entrapment capacity of hydrogels can be determined by the use of superparamagnetic nanoparticles. The MNPs concurrently act as a user defined biomolecule replacement and as a signal probe. MNPs can be designed in size and functionality to match the special needs of the experiments. For example, pH robust MNPs can be used to investigate pH-sensitive hydrogels. Analyzing the magnetorelaxation curves, the amount of embedded MNPs can be determined with (3). In further experiments the release rate of the MNPs will be investigated.

Acknowledgment

This work was financially supported by the DFG via SFB 578.

References

[1] Heim E, Harling S, Pöhlig K, Ludwig F, Menzel H and Schilling M 2006 *J. Magn. Magn. Mater.* **311** 150
[2] Kamath K R and Park K 1993 *Adv. Drug Deliv. Rev.* **11** 59
[3] Satish C S, Satish K P and Shivakumar H G 2006 *Indian J. Pharm. Sci.* **68** 133
[4] den Mooter G V, Vervoort L and Kinget R 2003 *Pharm. Res.* **80** 303
[5] Ludwig F, Mäuselein S, Heim E and Schilling M 2005 *Rev. Sci. Instrum.* **76** 106102
[6] Eberbeck D, Hartwig S, Steinhoff U and Trahms L 2003 *Magnetohydrodynamics* **39** 77
[7] Ludwig F, Heim E, Mäuselein S, Eberbeck D and Schilling M 2005 *J. Magn. Magn. Mater.* **293** 690
[8] Berkov D V and Kötitz R 1996 *J. Phys.: Condens. Matter* **8** 1257
[9] Eberbeck D, Wiekhorst F and Steinhoff U 2006 *J. Phys.: Condens. Matter* **18** 2829
[10] Ludwig F, Heim E and Schilling M 2008 *J. Appl. Phys.* **103** 07A314
[11] Vlierberghe S V, Cnudde V, Dubruel P, Masschaele B, Cosijns A, Paepe I D, Jacobs P J S, Hoorebeke L V, Remon J P and Schacht E 2007 *Biomacromolecules* **8** 331